Non-linear Characteristics of an Optically Reconfigurable Microwave Switch

Alexander W. Pang, Souheil Bensmida, Chris D. Gamlath, Martin J. Cryan**

Department of Electrical and Electronic Engineering, University of Bristol, Bristol, BS8 1TR, U.K.
*alex.pang@bristol.ac.uk, m.cryan@bristol.ac.uk

Abstract: A novel, high power optically controlled microwave switch is presented. The switch uses integrated illumination of a silicon superstate through a low loss glass substrate which reduces losses related to the plasma conductivity tail in the silicon. Numerical electromagnetic modelling is used to design the switch and good agreement between measured and simulated results has been achieved. The switch is then characterised using a two-tone non-linearity test at 2GHz and a third order intercept point of +72dBm is obtained with 10W per tone.

1. Introduction

Recently, the coexistence of several wireless communication standards, combined with the use of several frequency bands, represents a challenge to radiofrequency (RF) circuit design [1]. Transceivers need to operate at an unprecedented number of frequency bands with a variety of complex RF signals. To tackle this problem, there has been a growing interest in designing tunable microwave circuits. Reconfigurable circuitry can reduce system size and cost by providing frequency tuning instead of duplicating the same circuits for every desired band. Mature reconfiguration techniques are mainly based on varactor diodes, PIN diodes and Radio-Frequency MicroElectroMechanical Systems (RF MEMS) [2-6]. Varactor and PIN diodes can be employed to provide low insertion loss and continuous frequency band tuning but cannot easily handle high power signals because of their diode non-linear behaviour [2-4]. RF MEMS switches give excellent isolation values and linear behaviour. However, there are issues with reliability and high power performance, in particular with "hot-switching" [5-6]. One overriding issue with all these approaches is the requirement for DC bias lines. At low microwave frequencies, this is not a major issue for simple switching/tuning networks, but with many 10's-100's of elements this can become very complex. However, at millimetre wave frequencies and beyond, the requirement for complex DC biased networks can severely limit system performance. Optically tunable devices remove the need for bias circuits and since no diode junction or Schottky barrier is required within the structure, very linear performance should be achievable.

Thus, photoconductivity based tuning in a semiconductor, despite its relatively lossy behaviour [7], could be a strong candidate technology because of a number of important advantages. These include very high operating frequencies, with up to 266GHz operation having been shown [8], very linear performance [9] and good power handling capability [10]. An optically controlled photoconductive microwave switch has been demonstrated [10], where, the Third Order Intercept Point (TOIP) was measured as +63dBm referred to the RF output signal power in a single tone harmonic non-linearity test with a maximum 1W RF input power. In [11] input power of 25W was achieved in a single tone non-linearity test. This paper shows complete two-tone non-linearity results with 10W input power per tone which gives excellent performance similar to MEMS devices [5]. This paper also builds on the tunable antenna we developed in [12] where we introduced bottom side illumination through a glass substrate and applies this to a microstrip switch. Bottom side illumination through drilled conventional substrates has been shown previously [13], however the use of glass substrates minimises the discontinuity introduced into the microstrip line which will become much more important at higher frequencies where optically controlled switching becomes a very attractive technology. Our previous papers [7,11] performed low power, linear characterisation, this paper presents full non-linear characterisation of a switch.

The concept of optically reconfigurable microwave circuits has been described in detail in our previous work [7]. When an area of semiconductor is illuminated, it becomes electrically conductive, provided the photon energy is greater than the semiconductor band gap such that electron and hole pairs are generated and a plasma region is formed by the excess carriers [7]. The drawback of this technique is the requirement for considerable DC power for the light source. There are applications such as in Radar and mobile phone basestations where the requirement for 1-2W more of DC power will not overly effect the power budget of the system. There are also new device technologies such as microLEDs being developed that have very high optical intensities in very small areas leading to much lower DC power requirements [14].

This paper will firstly present the measured and simulated results for a bottom illuminated superstrate tuned microstrip gap line. Measured results are compared with Finite Integration in Time (FIT) based simulations in CST [15] and good agreement is obtained. Secondly, a two-tone non-linearity characterisation is performed with a maximum input RF signal power of 10W per tone at 2GHz. Finally, conclusions are drawn.

2. Fabrication and measurement setup

As mentioned above a key feature of this work is the use of a transparent low loss microwave substrate: fused silica glass. The silica is 500μm thick and double-side polished. The silica wafer was initially cleaned using solvents to remove dust and impurities on the surface, immediately after which the wafer was sputter coated with 5nm titanium and 350nm gold in an ambient argon atmosphere. This 5nm

titanium middle layer was employed to improve the adhesion between the gold and the fused silica. Then photoresist was spin coated on the wafer which was exposed through a mask to define the circuit. The photoresist was then developed and hydrofluoric acid and hydrochloric acid etches were used to remove the gold and titanium respectively. Fig. 1. shows a microscope view of a microstrip gapline with a linewidth of 1mm and a gap of 0.4mm.

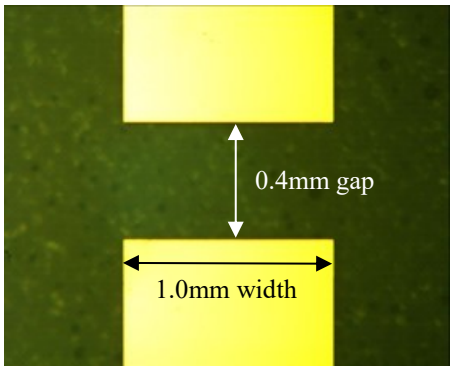

Fig. 1. *Microscope view of a 0.4mm gap in a 1mm wide microstrip line on fused silica glass*

Fig. 2 and Fig. 3 show the test circuit of the proposed optically tunable microwave switch. The fused silica glass substrate (ε=3.5) is mounted on a machined brass block. A piece of silicon, 5mm x 2mm x 0.5mm (ε=11.9) is used as a superstrate which is held in place using a thick perspex bar and two screws, and covers the microstrip gap. This superstrate silicon was a lightly doped n-type wafer with <100> orientation and resistivity $> 10K\Omega.\text{cm}$. A 300nm thick silicon dioxide layer is added to the bottom surface of the silicon in order to remove the Schottky contact between gold and silicon interface. Optical illumination is provided by a 980nm wavelength fibre coupled laser diode (Roithner Lasertechnik) this was chosen due to the high carrier generation efficiency at this wavelength. The fibre laser is coupled through a hole in the block which has been designed to have minimal effect on the microwave response. An electron-hole plasma region is generated in the silicon with the high conductivity region close to the microstrip gap. The lossy, lower conductivity tail is contained within the silicon and is then far from the high microwave field region in the gap and in the fused silica substrate, which substantially reduces losses compared to previous configurations [7].

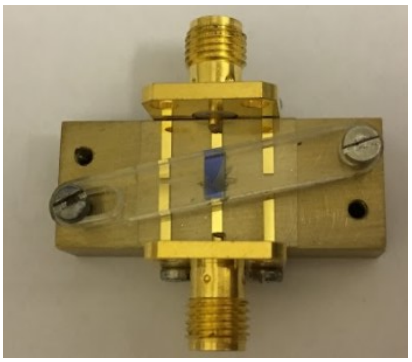

Fig. 2. *Top view of superstrate microstrip gapline with bottom illumination*

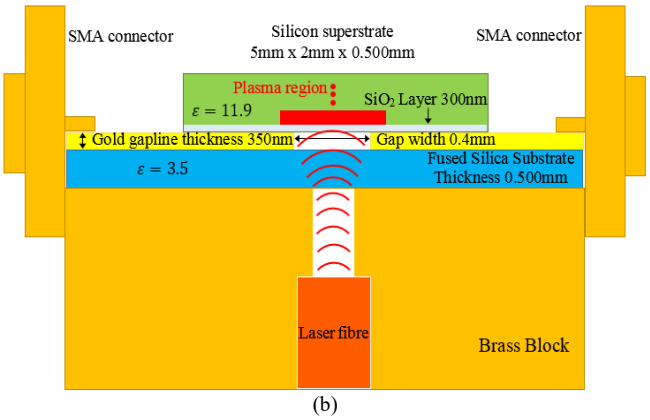

Fig. 3. *Schematic side view of superstrate microstrip gapline with bottom illumination*

3. Measurement and simulation

Fig. 4 shows the measured S_{21} for the microstrip gap under different illumination intensities which was achieved by varying laser drive power levels at a fixed laser spot size condition.

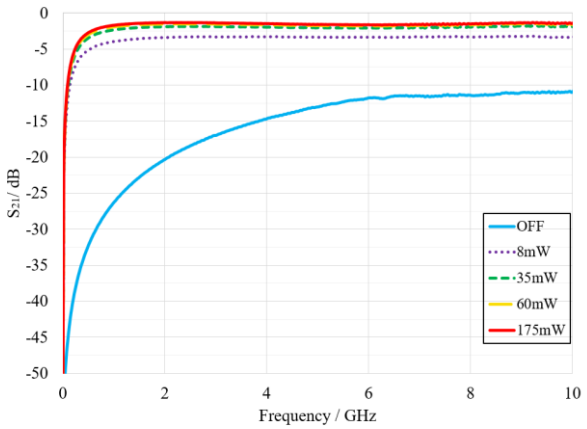

Fig. 4. *Measured S_{21} magnitude for 0.4mm gap 1mm linewidth superstrate microstrip gapline at varying laser power levels*

The no-light case (OFF) gives 20dB Isolation at 2GHz. With laser drive current just above the threshold, the corresponding illumination power, 8mW, results in a significant rise in S_{21}. It is clear that the transmission increases continuously as the laser power increases. Fig. 5 shows S_{21} at 2GHz vs. input optical power. It can be seen that there is a rapid increase in transmission with optical power upto 15mW, which then saturates at around 100mW. The maximum transmission is -1.3dB at 175mW optical input power.

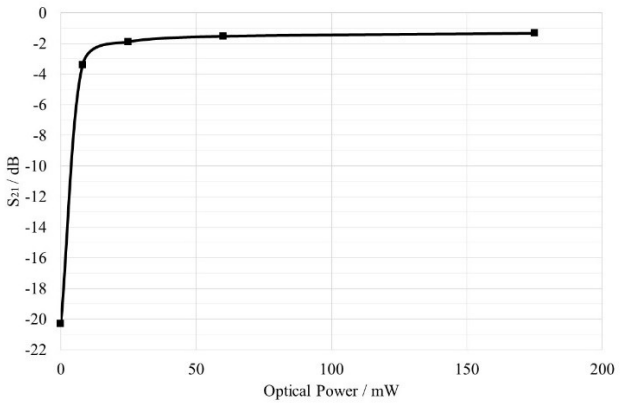

Fig. 5. *Measured S_{21} magnitude vs. optical power for 0.4mm gap 1mm linewidth superstrate microstrip gapline at 2GHz*

CST is used as a full wave 3D Electromagnetic modelling tool [15]. The plasma region can be represented by a series of varying conductivity layers as described in [7] and Fig. 6 shows the conductivity profile used in this work. The corresponding parameters are taken for absorption depth as 96µm [16], bulk recombination time as 10µs, diffusion length as 120µm [7]. Fig 7 shows the ten cascaded conductive layers derived from Fig. 6 In addition, a gap has been left between the gold layer and the bottom conductive layer of 10µm to simulate the metal-insulator-plasma contact transition and obtain good agreement at low frequencies. Currently the $Si0_2$ layer is not included in the model since this would require very fine meshing.

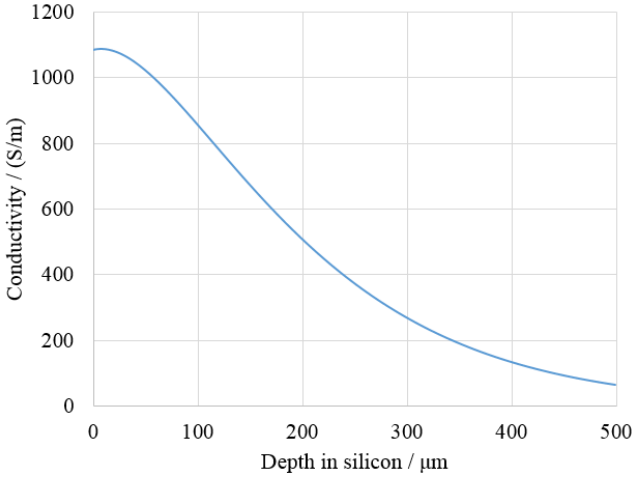

Fig. 6. *Conductivity vs. diffusion depth in silicon superstrate*

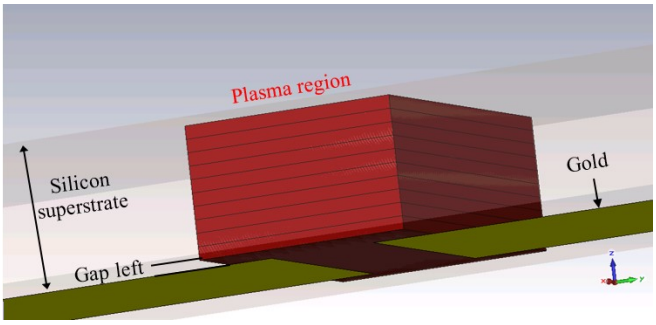

Fig. 7. *Plasma layers within silicon superstrate in CST view*

Fig. 8. shows good agreement has been achieved between measured and CST simulated results. The ON state conductivity has been chosen here in order to get the best fit to the measured results. Work is on-going to calculate this value directly from known optical input power based on the electrical properties of the silicon being used here.

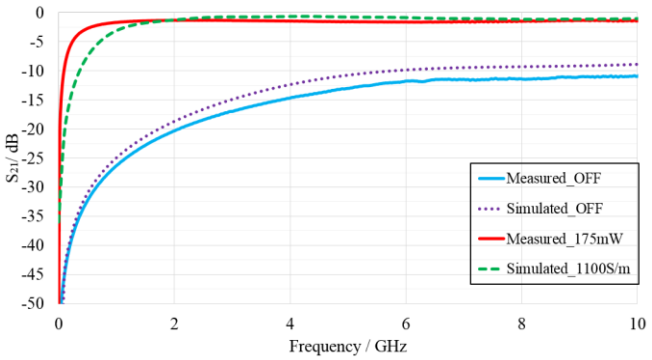

Fig. 8. *VNA measured and CST simulated results comparison at laser switched ON and OFF states*

4. Non-linear measurement

Large signal characterisation in the presence of a two-tone signal is performed to investigate the non-linear behaviour of the switch, in terms of intermodulation products, and its high power handling ability. The frequencies of these two tones are chosen as 2.000GHz and 2.001GHz on account of its employment in current wireless communication standard bands that vary from 1.4MHz to 20MHz. In this case we do not expect the frequency spacing to have an impact on the non-linear behaviour, as it does for active devices. In the future, we plan further two-tone measurements with different frequency spacing to confirm this.

Fig. 9 shows the two-tone non-linearity measurement set up. The two-tone signals were generated by two synchronised signal generators and combined after two linear amplifiers. This approach was taken since the use of a single driver with a two-tone generator at its input may result in the observation of the driver non-linear behaviour rather than that of the microwave switch.

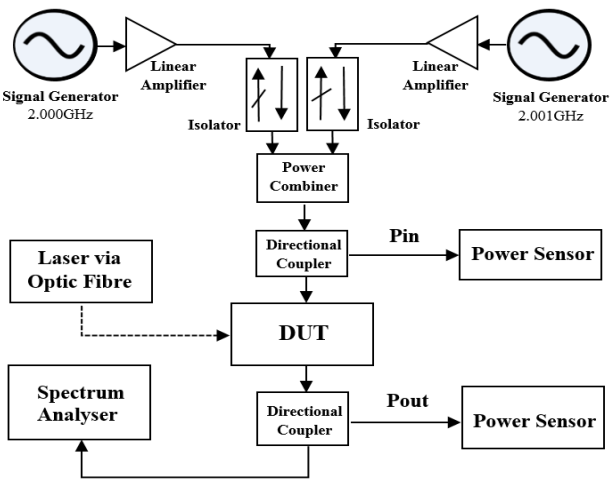

Fig. 9. *Non-linearity measurement schematic diagram*

Power meters were used to measure input and output power levels at the terminals of the microwave switch. As shown in Fig. 10 it is clear that there was no observable 3rd order InterModulation products (IM_3) when the total power of the two-tone input signal P_{in}, was increased up to +36.1dBm, (~4W).

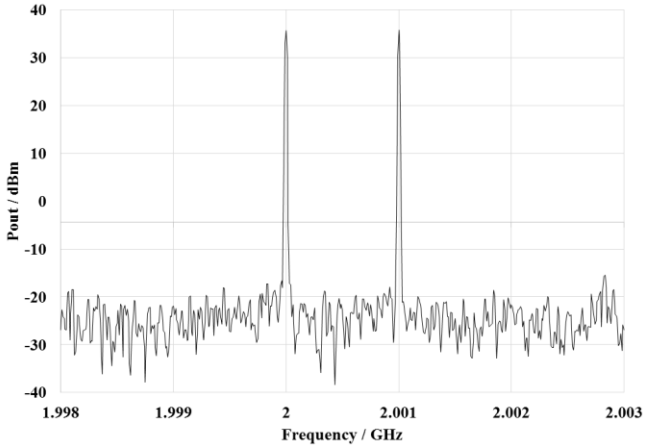

Fig. 10. P_{out} spectrum at P_{in} of 36.1dBm

Fig. 11 shows that when P_{in} is further increased to +43.0dBm (~20W), asymmetric IM_3 gradually appear which can be observed at 2.002GHz and 1.999GHz. At these very high power levels some melting of the perspex was observed and the contact between the silicon and gold track deteriorated. This could be a potential cause for the observed non-linear behaviour. These power levels are close to the maximum achievable with our current set up and the Third Order Intercept point referred to input power (IIP3) is estimated to be +72dBm in Fig. 12.

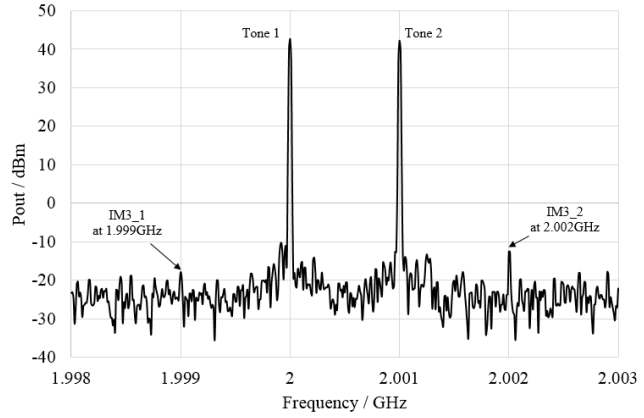

Fig. 11. *P_{out} spectrum at P_{in} of +43.0dBm*

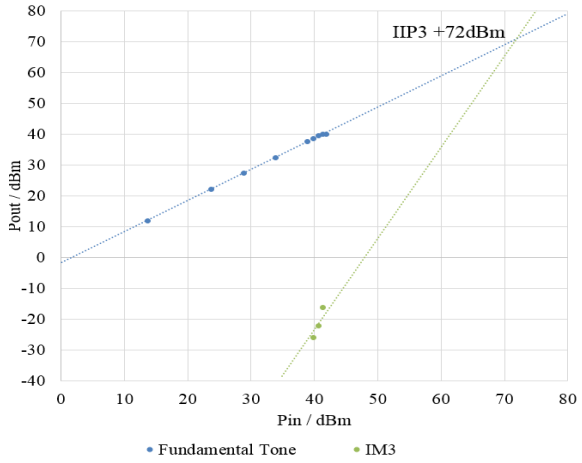

Fig. 12. *P_{out} vs. P_{in} with 3rd Intercept Point at +72dBm*

5. Conclusion

This paper presents a bottom illuminated optically controlled microwave switch with an insertion loss of 1.3 dB at 2GHz and an off-state isolation of 20dB. Good agreement with electromagnetic modelling has been shown. Input power has been increased to +43dBm in a two-tone measurement and IIP3 is predicted to be +72dBm. Optimisation of the microstrip gap geometry and collimation of laser will further improve the switch performance. The optically induced plasma used here is inherently frequency independent in nature and thus it is envisaged that millimetre wave performance of such devices will be equally good. This is particularly encouraging since conventional switching approaches become much more difficult to implement in those frequency ranges.

6. References

[1] Berezdivin, R., Breinig, R., Topp, R.: 'Next-Generation Wireless Communications Concepts and Technologies', *IEEE Communications Magazine*, 2002, **40**, (3), pp. 108-116

[2] Haupt, R. L., Lanagan, M.: 'Reconfigurable antennas', *IEEE Antennas Propagat. Mag.*, 2013, **55**, (1), pp. 49–61

[3] Christodoulou, C. G., Youssef, T., Steven A. L., *et al.*: 'Reconfigurable antennas for wireless and space applications', *Proc. IEEE*, 2012, **100**, (7), pp. 2250-2261

[4] Rauscher, C.: 'Reconfigurable bandpass filter with a three-to-one switchable passband width', *IEEE Trans. Microw. Theory Tech.,* 2003, **51**, (2), pp. 573-577.

[5] Patel, C.D., Rebeiz, G. M.: 'A high-reliability high-linearity high-power RF MEMS metal-contact switch for DC–40-GHz applications', *IEEE Trans. Microw. Theory Tech.,* 2012, **60**, (10), pp. 3096-3112

[6] Chow, L. L. W., Volakis., J. L., Saitou., K. *et al.*: 'Lifetime Extension of RF MEMS Direct Contact Switches in Hot Switching Operations by Ball Grid Array Dimple Design', *IEEE Electron. Device Lett.,* 2007, **28**, (6), pp. 479-481

[7] Gamlath, C. D., Benton, D. M., Cryan, M. J.: 'Microwave Properties of an Inhomogeneous Optically Illuminated Plasma in a Microstrip Gap', *IEEE Trans. Microw. Theory Tech.,* 2015, **63**, (2), pp. 374-383

[8] Kulygin, M., Denisov, G., Vlasova, K., *et al.*: 'Nanosecond Microwave Semiconductor Switches for 258… 266 GHz', *Journal of Infrared, Millimeter, and Terahertz Waves*, 2015, **36**, (9), pp. 845-855

[9] Kaneko, T., Takenaka, T., Low, T.S., *et al.*: 'Microwave switch: LAMPS (light activated microwave photoconductive switch)', *IEEE Electronics Letters*, 2003, **39,** (12), pp. 917-919

[10] Kowalczuk, E.K., Panagamuwa, C.J., Seager, R.D., *et al.*: 'Characterising the linearity of an optically controlled photoconductive microwave switch', *In Antennas and Propag. Conf. (LAPC)*, Loughborough, U.K., November, 2010 pp. 597-600

[11] Kowalczuk, E.K., Seager, R.D., and Panagamuwa, C.J.: 'Power handling of a photoconductive microwave switch', *In Antennas and Propag. Conf. (LAPC)*, Loughborough, U.K., November, 2016 pp. 1-3
[12] Gamlath, C. D., Collett, M.A., Pang, A.W., *et al.*: 'Investigation of an optically induced superstrate plasma for tuning microstrip antennas', *IET Optoelectronics*, 2017, **11**, (6), pp. 230-236
[13] Youssef, T., Joseph, C., Sameer, H., *et al*.: 'Demonstration of a cognitive radio front end using an optically pumped reconfigurable antenna system (OPRAS)', *IEEE Trans. on Antennas and Propag*., 2012, **60**, (2), pp. 1075-1083
[14] Jeorrett, A.H., Neale, S.L., Massoubre, D., *et al*.: 'Optoelectronic tweezers system for single cell manipulation and fluorescence imaging of live immune cells', *Optics express*, 2014, **22**, (2), pp. 1372-1380.
[15] CST Microwave Studio 2015, Computer Simulation Technology, 2015, https://www.cst.com/
[16] Green, M. A., Keevers, M. J.: 'Optical properties of intrinsic silicon at 300 K', *Progress in Photovoltaics: Research and Applications*., 1995, **3**, (3), pp. 189-192